This is a pre-print of an article published in *Landslides.* The final authenticated version is available online at: 10.1007/s10346-018-1031-z

AQ1

Deep-seated gravitational slope deformations triggered by extreme rainfall and agricultural practices (eastern Michoacan, Mexico)

Cecilia Irene Villaseñor-Reyes, [1]✉

Phone +52-4432855384
Email cecilia.villasenor@ipicyt.edu.mx

Pablo Dávila-Harris, [1]

Víctor Manuel Hernández-Madrigal, [2]

Sócrates Figueroa-Miranda, [1]

[1] División de Geociencias Aplicadas, IPICYT, Camino a la Presa San José 2055, Lomas 4ta sección, 78216 San Luis Potosí, Mexico

[2] Instituto de Investigaciones en Ciencias de la Tierra, UMSNH, Avenida Francisco J. Mujica S/N, 58030 Morelia, Mexico

Received: 30 March 2018 / Accepted: 21 June 2018

Abstract

The study of deep-seated gravitational slope deformations (DSGSD) in Mexico is scarce; therefore, their localization and causes are highly overlooked. The present paper examines the characterization of the DSGSD of Jungapeo and Las Pilas in eastern Michoacan state, currently active and endangering their inhabitants. An integrated study, including detailed lithology, morpho-structural inventories, analysis of land use, and pluviometric regime, was performed and complemented with differential global positioning system monitoring networks. Both landslides developed over highly weathered volcano-sedimentary rocks. On the one hand,

the Jungapeo landslide has an estimated volume of 990,455 m^3 with steady decreasing velocity rates from 41 to 15 cm/month in the first monitoring period to 13–3 cm/month in the last one. On the other hand, the Las Pilas landslide estimated volume is about 1,082,467 m^3 with a stable velocity rate of 1.3 to 0.1 cm/month. Despite the multi-storeyed style of activity, two behaviors of instability were distinguished: slow deformation and secondary landslide stages. The conditioning factors for slow deformation in both DSGSD are the combination of weathered lithology with clay- and sand-rich content, and the shift toward intensive monoculture. The triggering factor is related to excess water produced by an inefficient flood-irrigation system that also generates an atypical acceleration behavior in both landslides during the dry season. The DSGSD activity thus predisposes the generation of tension cracks and secondary scarps from which the collateral landslides are triggered by atypical rainfall, such as that of 2010.

Keywords

Deep-seated gravitational slope deformations
Kinematic behavior
Landslides
Michoacan
Mexico

Introduction

Deep-seated gravitational slope deformations (henceforth DSGSD) has been recognized worldwide (Pánek and Klimeš 2016). Yet, in Mexico, the identification, research advances and inventory of these phenomena have remained limited (Muñiz-Jauregui and Hernández-Madrigal 2012). However, after a series of atypical rains in February 2010 (Aguilar-Garduño et al. 2010; Figueroa-Miranda 2013), two independent slopes in eastern Michoacan state have gained attention due to the slow deformation that have affected local buildings, roads, and crop fields. These hill slopes are located in a highly active agricultural area, endangering two communities within the Jungapeo municipality (Fig. 1). The first community, Jungapeo town, located in the central part of the municipality, has 5073 inhabitants and 1533 households (INEGI 2010a). The other community, Las Pilas, 4 km away, located in the eastern part of the municipality, has 174 inhabitants and around 50 households (INEGI 2010a).

Fig. 1

General location map of the study area, (a) within Mexico and (b) in eastern Michoacan state. Stars in (b) indicate the Active National Geodetic Network stations used in differential GPS correction. (c) Hillshade map showing the extension of the deep-seated gravitational slope deformations in Jungapeo and Las Pilas. The black star in (c) indicates the location of the weather station used for rainfall analysis

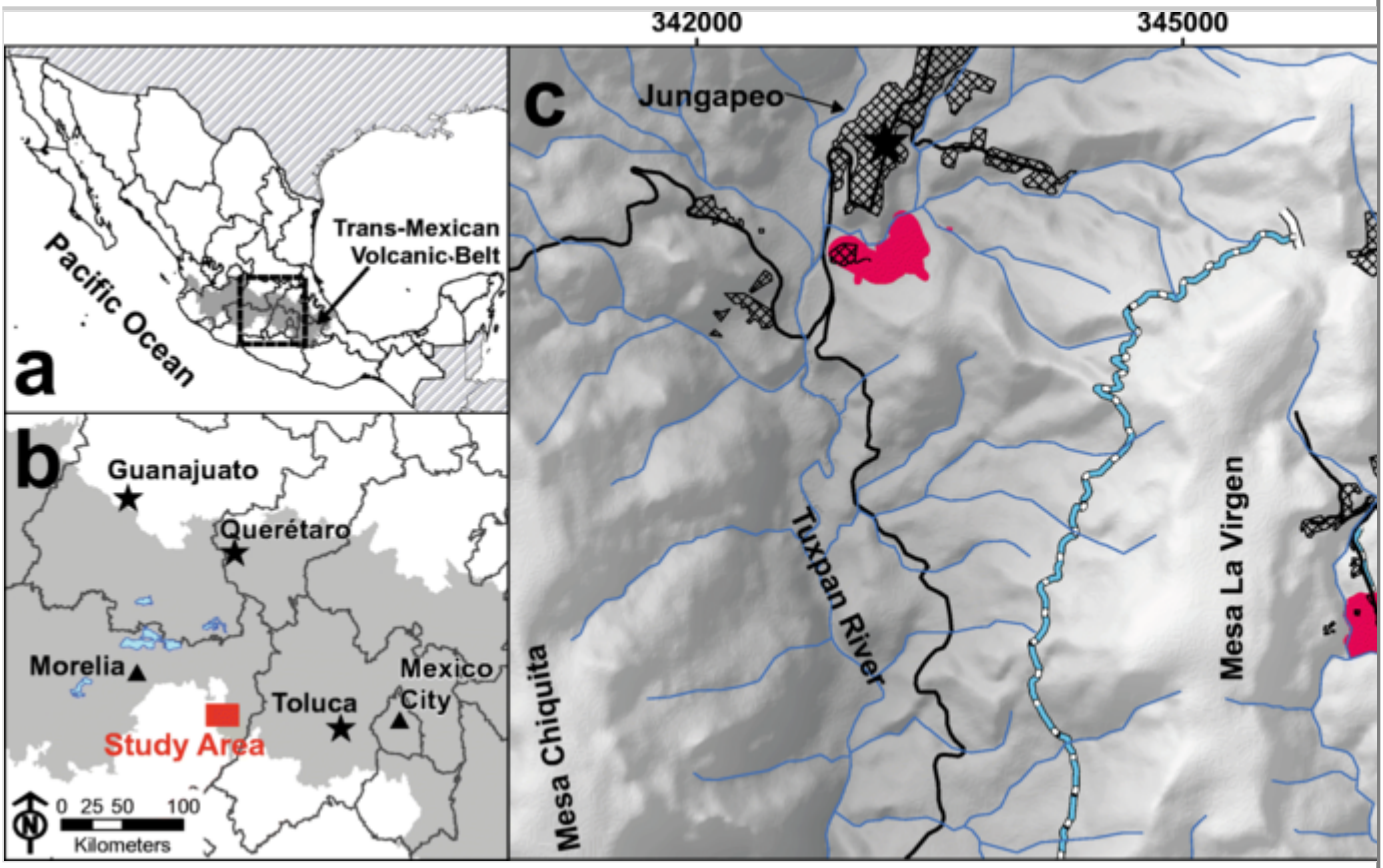

History of local instability in the area dates back over decades, with clear acceleration or reactivation by the abovementioned 2010 hydro-meteorological event. Nonetheless, these kinds of instability processes have never been thoroughly studied in Mexico. Thus, the objective of this paper is to characterize the temporospatial extension and behavior of the two phenomena. The paper also seeks to address the triggering factors and the influence of rain and land use in the acceleration of the slow movement and generation of secondary mass movements, principally to identify anomalous behavior in the movement patterns that potentially lead to disastrous consequences. Therefore, monitoring networks based on differential global positioning system (henceforth DGPS) were implemented to make for a better understanding of the kinematics of the slopes. The monitoring technique was supported with geological analysis of the area, local mass movement

inventory, morpho-structural maps, analysis of the land use, and pluviometric regime.

Methodology

Geological setting of the area was updated from published papers and unpublished technical reports through orthophotos (2 m in resolution), hillshade maps (15 m in resolution), and field surveys. These data were used to describe the lithology, define the contacts and strata disposition of each unit involved on the slopes. Also, to provide a better understanding of the processes in the unstable areas, geological cross sections were produced.

Using two image sets, morpho-structural and land use maps of each slope were produced. The first set comprised satellite images from 2002, 2010, and 2016, available on Google Earth™ platform. Additionally, for the Jungapeo instability area, we used two images taken by an unmanned aerial vehicle (UAV) in 2014 and 2015 (10 cm in resolution). These image sets allowed the characterization of the main scarps, body limits, secondary scarps, tension cracks, active detachment zones, and differentiation of the crop type. All the derived information was verified by using field surveys.

To determine the extension of each landslide and its topographic displacements, we carried out six DGPS survey campaigns. The field campaigns started in June 2013, in Las Pilas and in March 2015, in Jungapeo, lasting in both locations until February 2017. During these operations, we used a Leica differential GPS, SR500 model with 12 channels and dual frequency. On the one hand, the Las Pilas monitoring network consisted of a base station located at the school named “16 de septiembre” and of ten topographic control points within the affected area we measured throughout the campaign. On the other hand, the monitoring network in Jungapeo comprised a base station located in the high school named “CBTA 240” and of 13 topographic control points. Of the latter, only four (J3, J7, J8, and J10) were measured during all of the monitoring campaigns; points J4, J11, and J12 were added in April 2015, while three more (J5, J9, and J13) presented problems in their precision values in one or more of the campaigns. Finally, three points were removed because of the construction of a basketball court (J1 and J2 in early 2017) and the constant deformation of the slope (J5 in mid-2015). Using the Active National Geodetic Network (RGNA) stations of Guanajuato, Querétaro and Toluca (Fig. 1(b)), the base station coordinates of both locations were corrected. For each control point and according to the Technical Standard for Positional Accuracy (INEGI 2010b), the standard deviations, circular error probability (CEP), and

vertical position uncertainty (EPV) were calculated. Through data processing, the accumulated deformation, monthly velocity and displacement vectors were calculated.

For the analysis of the pluviometric regime, we utilized the weather station closest to the landslides. The 16058 CONAGUA (National Water Commission) station is located 700 m from the Jungapeo landslide and four kilometers from the Las Pilas landslide (Fig. 1(c)). The station has 72 years of collected data (1943–2015). However, this number reduced to 26 years (1943–1947, 1951, 1961, 1964–1969, 1971, 1974–1976, 1979–1981, 1984, 1989, 2009–2012) since they were the only ones with information for all the months in each of these years. Further, we added three incomplete years (2013–2015) to include the most recent information concerning the area. Monthly average rainfall and rainy days were calculated for the periods 1943–2009 and 2011–2015. With this array, we were able to analyze what the rainfall behavior was like before and after the atypical event of 2010, for which the values for the same variables were also calculated. Moreover, the correlation between the deformation behavior obtained with the DGPS and the semi-annual rainfall regime of the area was compared.

Results

Local geology

The study area is located in the southeastern part of the central sector of the Trans-Mexican Volcanic Belt (henceforth TMVB) (Fig. 1(a)). Stratigraphically, the local basement is formed by Upper Jurassic to Lower Cretaceous volcano-sedimentary deposits of the Guerrero terrain (Israde-Alcántara and Martínez 1986; Pasquarè et al. 1991) capped by basaltic products of the TMVB. This stratigraphic succession is highly dissected by north-south steep river canyons that follow trending faults (Blatter and Carmichael 1998) and form a local relief difference of 600 m with slope values up to 56°.

Locally, four lithostratigraphic units were recognized in Jungapeo (Figs. 2 and 3(a)). Their details are presented, from base to top, as follows:

Fig. 2

Local lithological map of the study area. ZVC Zitácuaro volcanic complex. Ages taken from Aguirre-Díaz et al. 2006; Garduño et al. 1999; Israde-Alcántara and Martínez 1986

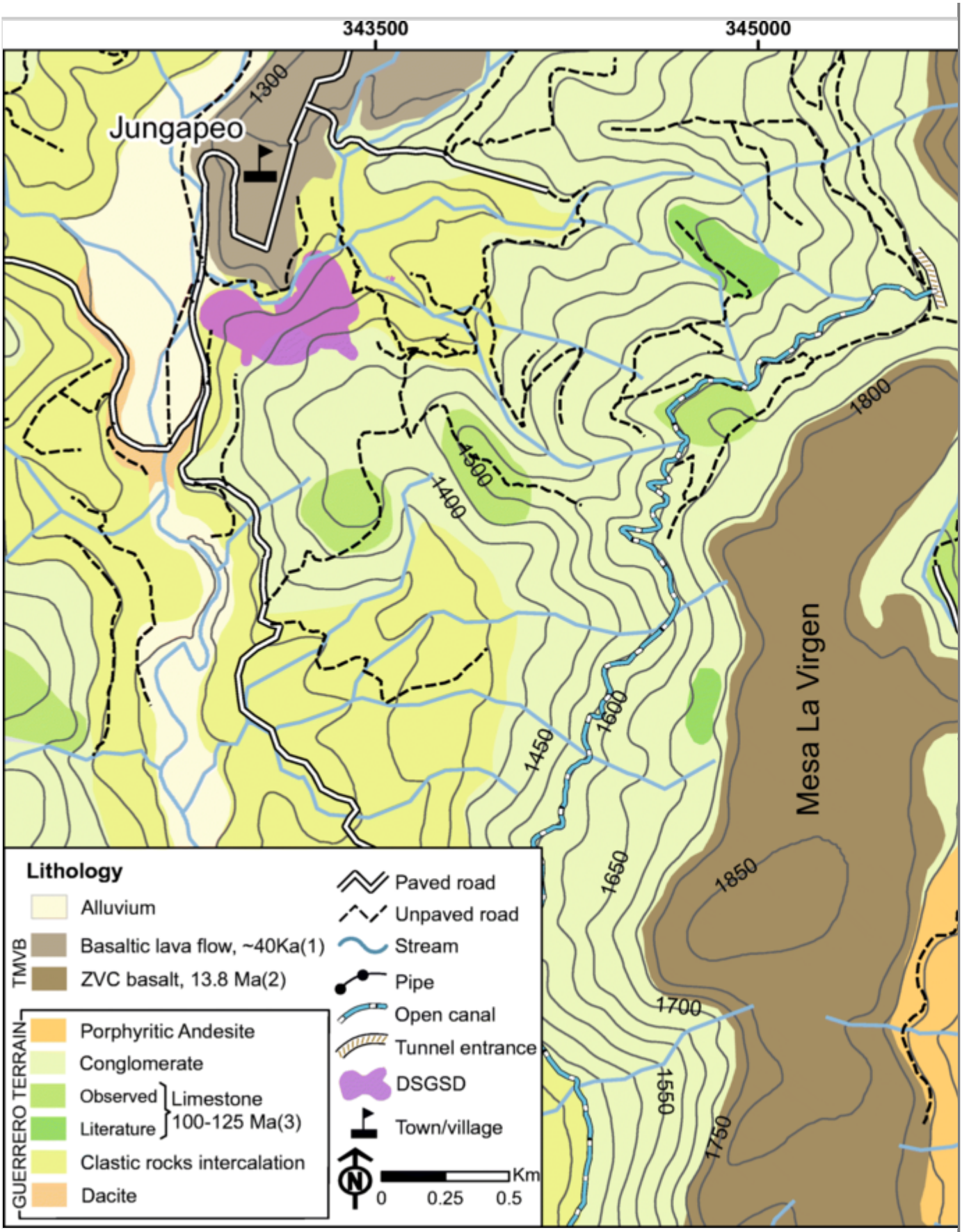
343500
345000
Jungapeo
1300
1400
1450
1500
1550
1600
1650
1700
1750
1800
1850
Mesa La Virgen
Lithology
Alluvium
TMVB
Basaltic lava flow, ~40Ka(1)
ZVC basalt, 13.8 Ma(2)
GUERRERO TERRAIN
Porphyritic Andesite
Conglomerate
Observed
Literature
Limestone
100-125 Ma(3)
Clastic rocks intercalation
Dacite
Paved road
Unpaved road
Stream
Pipe
Open canal
Tunnel entrance
DSGSD
Town/village
N
Km
0
0.25
0.5

Fig. 3

Local stratigraphy of the Jungapeo area. (a) Schematic stratigraphic column of the four lithological units exposed in the Jungapeo area, including a dacite, overlain by a thick alternating sequence of shale, sandstone, and limestone, followed by a conglomerate package and younger basalt lava. (b, c) Textural variations of the sedimentary sequence

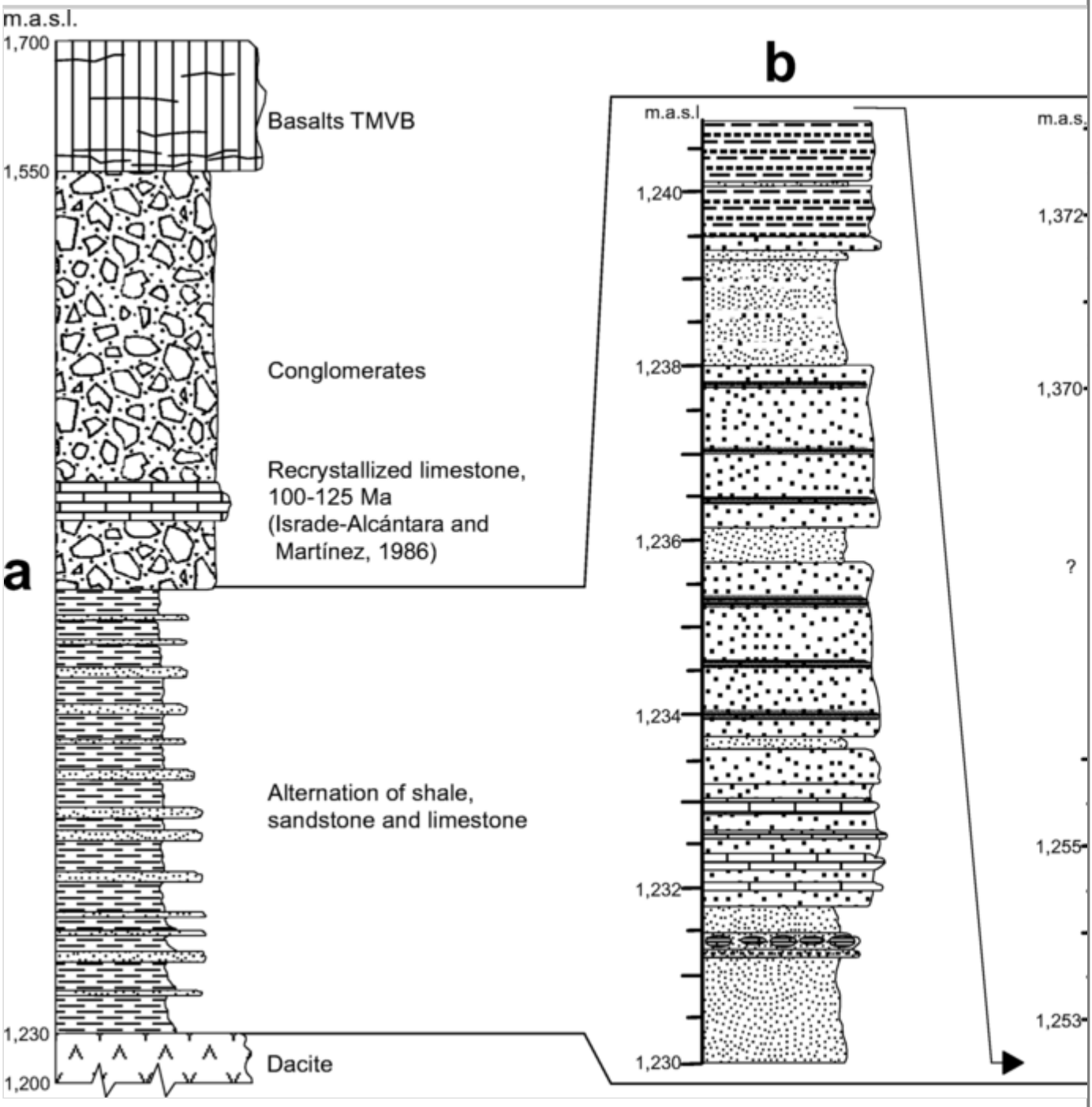

Dacite (Fig. 4(a)) This unit is only exposed in the western part of the area, at the base level of the Tuxpan River. It is highly weathered and fractured with a surface

exposure of more than 6 m thick.

Fig. 4

Lithostratigraphic units in the Jungapeo area. (a) Fractured and highly weathered basal dacite. (b) Alternation of bedded sandstone, shale, and limestone. (c) Upper folded sandstone and shale. (d) Altered polymictic conglomerate. (e) Monolithologic conglomerate. (f) Miocene basalts unconformably overlying the monolithologic conglomerate. (g) Mid-Pleistocene basalts and basaltic breccias

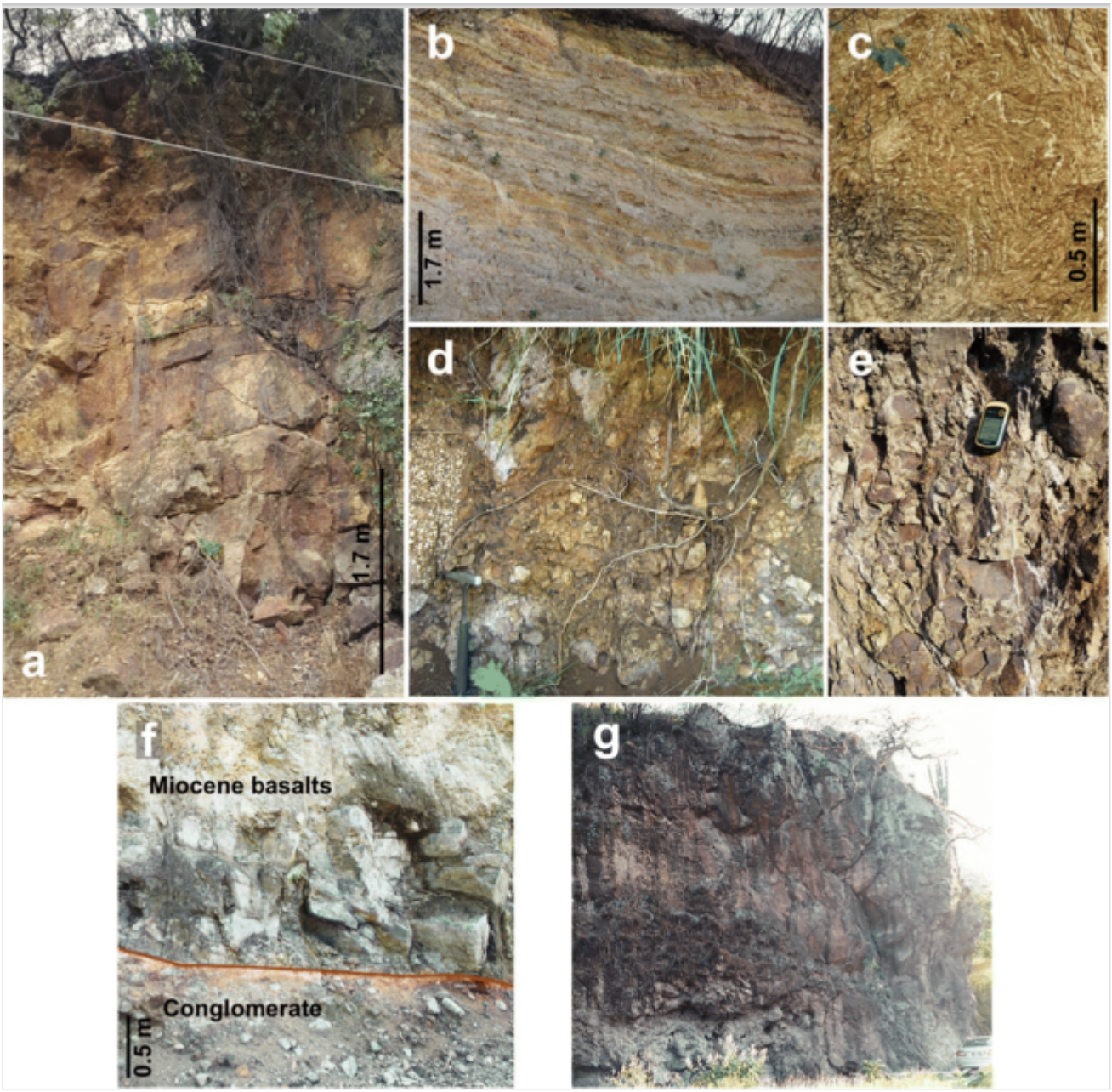

Sandstone, shale, and limestone This alternation (Figs. 3(b) and 4(b)) begins at 1230 m above sea level (m.a.s.l.) with a fine-grained laminar sandstone, poorly consolidated and calcite nodule interbeds. Upwards, there is a transition to well consolidated medium-grained sandstone with alternating limestone levels (~ 12 cm) that in turn are replaced by coarse-grained sandstone beds ~ 20 cm thick. At approximately 1239 m.a.s.l., this predominance of sand decreases and alternates with shales that ultimately form poorly consolidated laminar packages with oxidation (1253 m.a.s.l.) (Fig. 3(c)). Finally, the uppermost part of this sequence is folded and consists mainly of shale with coarse sandstone interbeds (Fig. 4(c)). The landslide body material, affected by continuous deformation and collateral landslides, is stratigraphically related to this unit and is composed of residual rock and piedmont in matrix of fine sand to clay.

Conglomerates This unit is formed by two members that unconformably overlie the previous sedimentary sequence. The first member is a poorly sorted and consolidated polymictic conglomerate (Fig. 4(d)) with interbeds of sandstone and recrystallized limestone of up to 2 m thick. It is matrix-supported and has sub-angular to sub-rounded clasts of limestone, basalt, andesite, and rhyolite, with sizes that range from a few centimeters to up to 1 m in diameter. The other member is a monolithologic clast-supported conglomerate (Fig. 4(e)). Its sub-rounded clasts are highly weathered basalt with sizes up to 30 cm in diameter. Recrystallized limestone lenses, which are up to 60 m across, are associated with this conglomerate.

Basalt The oldest volcanic products of the TMVB activity in the area correspond to the Miocene basaltic mesas of the Zitácuaro Volcanic Complex, to the west mesa Chiquita and to the east mesa La Virgen (Fig. 1(c); Garduño et al. 1999). They consist of aphanitic basalts with scarce subhedral pyroxene phenocrysts and minor vesicular texture that unconformably overlie the conglomerates (Fig. 4f). The town of Jungapeo is settled over Mid-Pleistocene monogenetic volcanism of the TMVB. These deposits consist of aphyric, vesicular basalt lava, and basaltic breccias that flowed down the river canyons, separating the mesas and partially burying the volcano-sedimentary deposits (Figs. 2 and 4(g); Blatter and Carmichael 1998).

In the Las Pilas area, four lithostratigraphic units were also identified (Figs. 2 and 5). Their details are presented, from base to top, as follows:

Fig. 5

Schematic stratigraphic column of the Las Pilas area, showing conglomerate overlain by recrystallized limestone. The top of the sequence is formed by Miocene and

Pleistocene basaltic lavas. (a) Highly altered volcanic breccia and (b) limestone bank

Conglomerate The north and south of this area are characterized by the presence of a highly weathered, monolithologic, and clast-supported conglomerate, ~~and~~ correlated with the one in Jungapeo area. This conglomerate also has sub-rounded basalt clasts with sizes up to 30 cm across.

Volcanic breccia This unit consists of sub-angular clasts of porphyritic andesite up to 30 cm long immersed in a matrix of reddish clay-fine sand (Fig. 5(a)). The Las Pilas affected area is emplaced within this unit.

Limestone This unit is formed by lenses of recrystallized limestone always associated, and in transitional contact, with the volcanic breccia and conglomerates. The size of the lenses increases to the upper part of the column until it forms limestone banks, up to 100 m thick (Fig. 5(b)). They also show the presence of intraformational breccia with very angular andesitic fragments, sand levels, and calcareous fragments (Israde-Alcántara and Martínez 1986).

Basalt To the west, the Miocene products of the TMVB form mesa La Virgen. It consists of aphanitic basalt with little pyroxene crystals and scarce vesicular texture. The eastern lava flow from the Zacapendo volcano corresponds to the Mid-Pleistocene TMVB activity, and it has vesicular aphyric texture (Fig. 1(c); Aguirre-Díaz et al. 2006). Both basalts cap all of the previous sequence.

Jungapeo landslide

General characteristics and morphology

The Jungapeo landslide develops in a northwest-facing slope. It encompasses an area of approximately 16.7 Ha, and at its toe, it has a secondary stream from the Tuxpan River. Its maximum width and length are 530 and 460 m, respectively, with a local relief difference of 160 m (1,230–1390 m.a.s.l.). Taking into account the depth of the several main scarps from the collateral landslides within the DSGSD limits (described below), a minimum volume of mobilized mass is estimated to be about 990,455 m^3.The central part of the area has a slope of 26°–40° whereas that of the left and right flanks range from 2° to 25°.

The morpho-structural analysis enabled the identification of several active detachment zones and 25 secondary shallow landslides (Fig. 6), thus classifying the activity style as multi-storeyed (Ter-Stepanian 1977). Figure 6 shows the three generation phases of collateral landslides identified. The oldest stage (purple polygons) marks the current boundaries of the main landslide. It contains three large avalanches up to 400 m long and three smaller landslides. Additionally, several scarps with northwest and northeast orientation, likely correspond to collateral landslides that cannot be constrained because of the erosion of their morphological features. However, during 2002, a second stage (Fig. 6, green polygons) produced tension cracks, two debris flows (48 m in length and a scarp depth of 5 m), and a translational slide (67 m in length and a scarp depth of 10 m), whose limits were later destroyed. The most recent phase (Fig. 6, red polygons) began after the 2010 heavy rainfall. The collateral landslides identified were five debris avalanches (150 m in length and scarp depths of 15 to 20 m; (c) in Figs. 6 and 7), ten rotational and translational slides (50 m in length and scarp depths of 5 to 10 m; (d) in Figs. 6 and 7), as well as one debris flow.

Fig. 6

Inventory and morpho-structure map of the Jungapeo landslide. Numbers (1–5) and letters (a, c, d) denote features referred to in the text and in Fig. 7

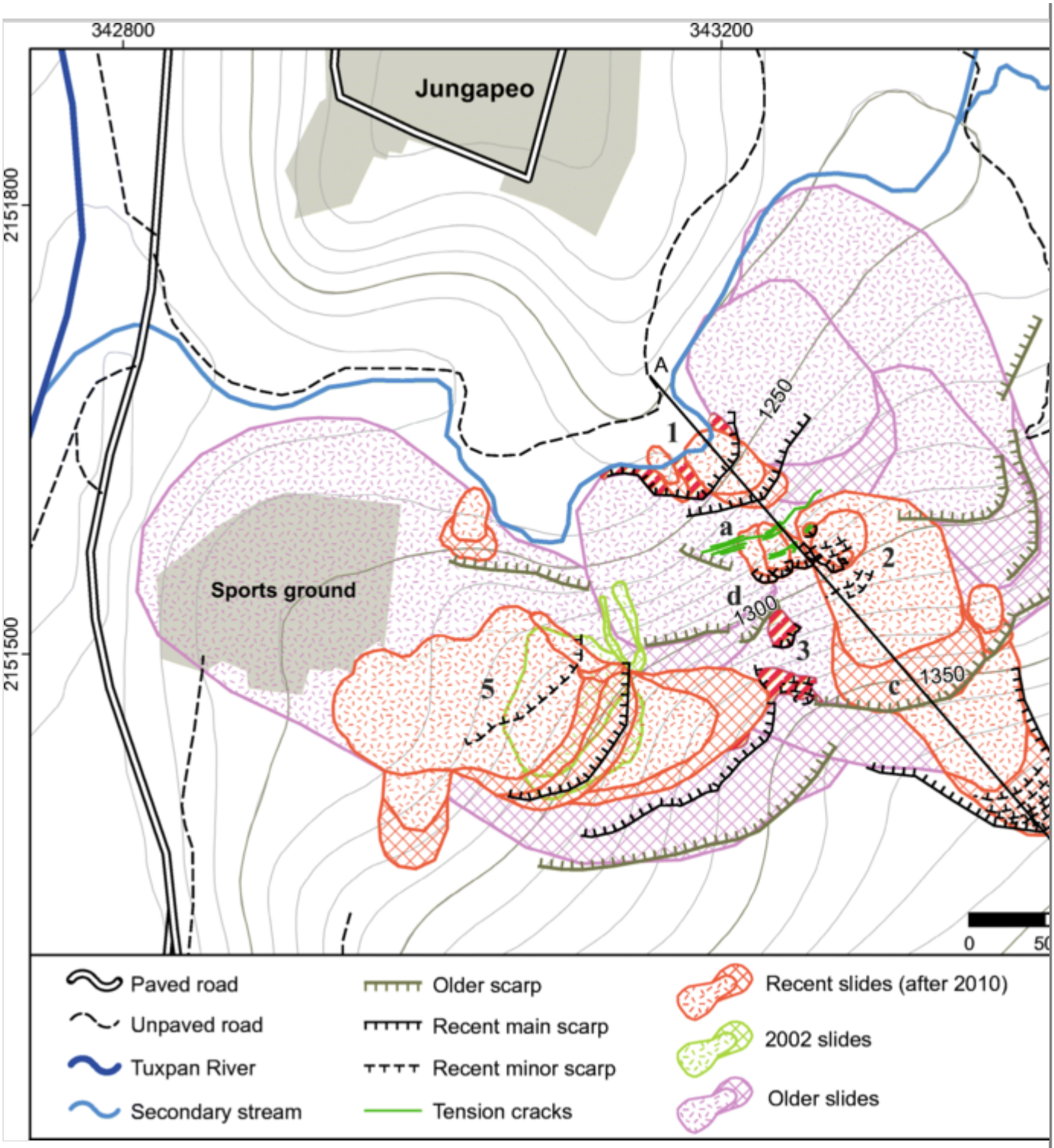

Fig. 7

Morpho-structure evidence of diverse deformation phases in the Jungapeo landslide. (a) Tension cracks on the central part of the affected slope in early 2016 and (b) its evolution for early 2017, more than 1 m opening. (c) Scarp of secondary landslide generated after the 2010 rain event, nearly 10 m high. (d) Two secondary landslide scarps of different deformation phases (the older one in the background and the younger in the foreground). The 3D figure was produced overlapping the unmanned

aerial vehicle image from 2015 and a digital elevation model (15 m in resolution). The bluish colors highlight the vegetation zones

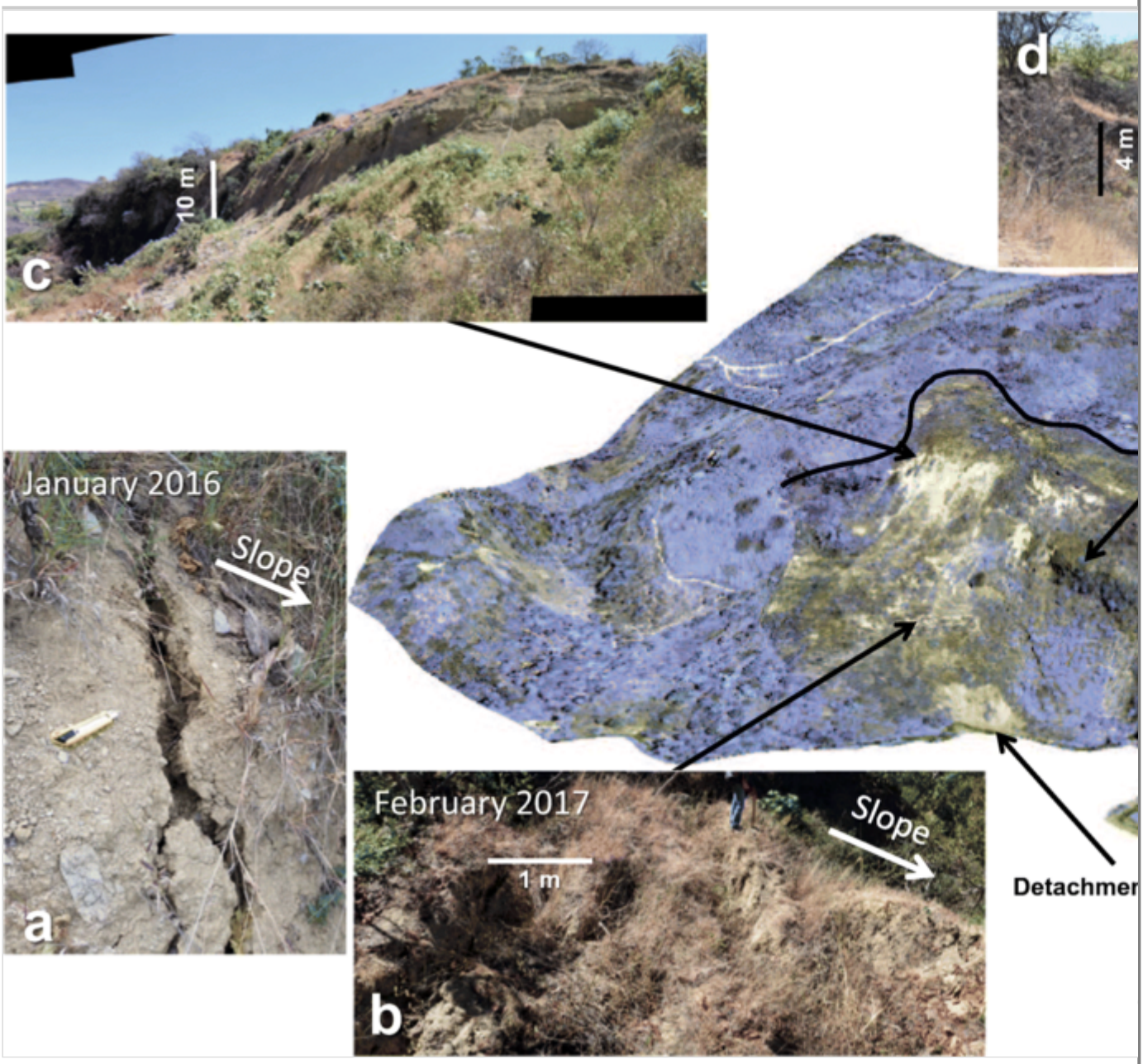

Currently, the slow deformation has promoted the development of tension cracks ((a) in Fig. 6) and secondary scarps with a NE-SW orientation in the middle and upper parts of the slope ((2–5) in Fig. 6). In 2016, the width of the main tension crack was approximately 15 cm increasing to more than 1 m wide and about 80 cm deep by 2017 ((a and b) in Fig. 7). These cracks are located directly on top of an active retrogressive detachment zone, promoted by stream erosion at the foot of the slope ((1) in Fig. 6).

Land use and affectations

As regards, the affected part of the slope surface, 84.4% is covered by low sub-deciduous forest (8.6 Ha) and pastureland (5.5 Ha) (Fig. 8). The latter is mainly concentrated in areas with recent collateral landslide activity (2002 to date). The central part of the slope represents a remnant of a guava crop (1 Ha) with a drip-irrigation system. After the generation phase of collateral landslides in 2010, these crops lost more than two thirds (2.4 Ha) of their original extension ((A) in Fig. 8). Further, above the crown of the landslide, the slope has a strong agricultural activity with a flood-irrigation system ((B) in Fig. 8) that was also partially affected by the development of an avalanche. It is worthy of note here that the sports ground located on the lower left flank (1.6 Ha) was also damaged by that time ((C) in Fig. 8).

Fig. 8

Land use and DGPS monitoring network (J2–J14) in the Jungapeo landslide. The size of the displacement vector is proportional to its accumulated movement (black arrows). Letters (A–C) denote features referred to in the text

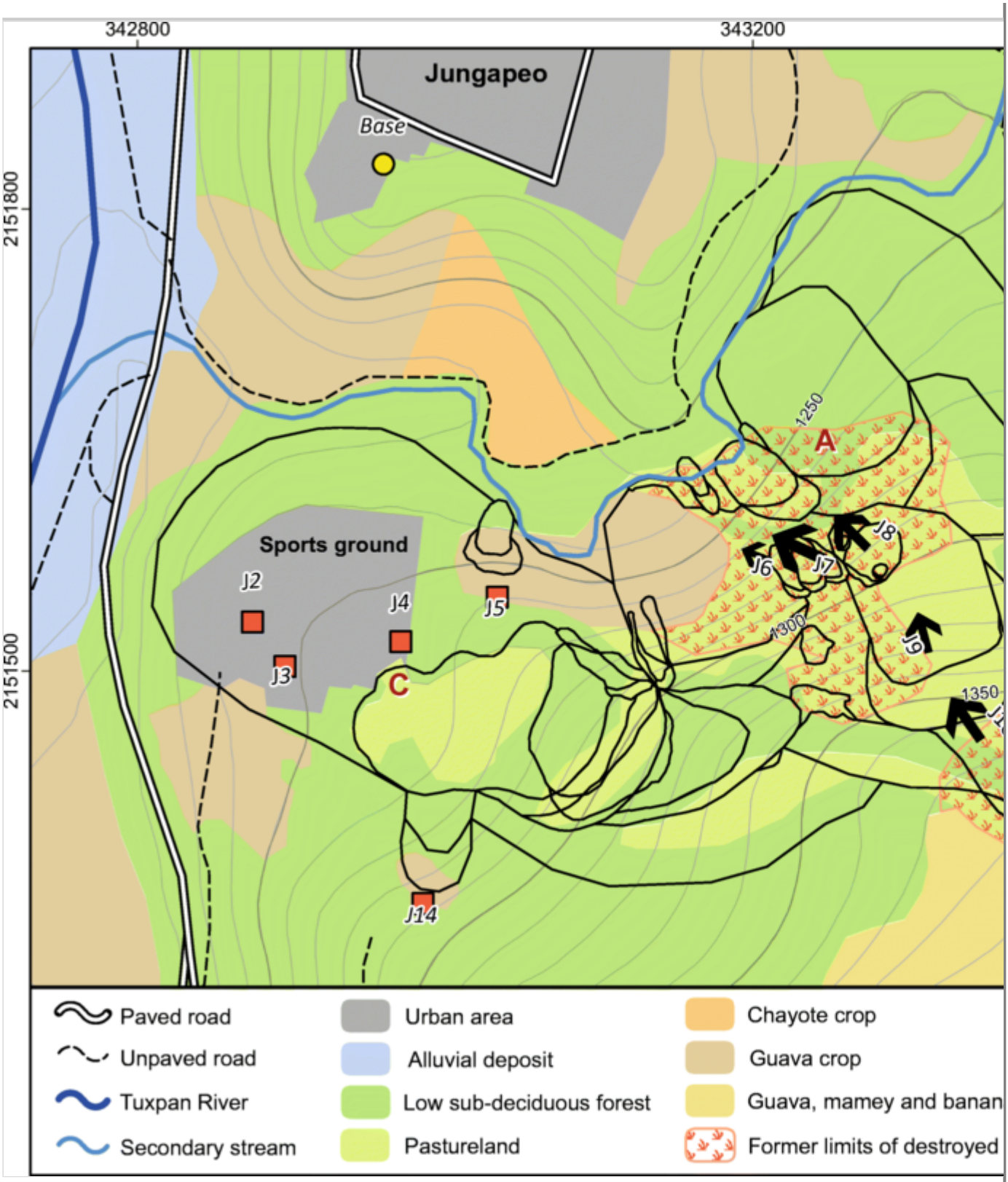

Surface deformation

Control points J2–J5 from the DGPS survey, positioned on the sports ground and the surrounding area, remained virtually stable (Fig. 8). In like manner, J12, J13, and J14, placed as reference points on a relatively stable terrain, do not show

deformation. These points helped to confirm that the displacements do not extend beyond the current limits established in Fig. 6. The main deformation recorded is located in the central part of the slope (J6–J11). The direction of the displacement vectors (N300° for J6–J8, N345° for J9, N320° for J10 and J11) is parallel to the slope-dip direction and almost perpendicular to the recent tension cracks and secondary scarps.

The accumulated displacement values show that all points had vertical and horizontal movements, the latter being predominant in all cases (Fig. 9(a)). Horizontal and vertical displacement rates appear to be gradually and steadily decreasing (Fig. 9(b, c)). The horizontal rates for the first monitoring period (41–15 cm/month) decreased by at least three times its rate, as compared with the last monitoring period (13–3 cm/month). The rates for vertical values had a similar result with 19–12 cm/month for the first period and 6–2 cm/month in the last period. Furthermore, all points have a cyclical behavior that is more notorious on the horizontal component and in which the displacement rate has an increase in the first half of the year and a decrease by the second half.

Fig. 9

This may not be allowed by the format of the journal, but figures 9, 13, and 14 could be adjusted to one-column size and put it them along the column text to save space.
In any case, figures 9, 13, and 14 were made to be smaller. If the previous suggestion is not allowed or it is not clear, then it would be helpful to reduce the size of these images if you consider it necessary.

DGPS monitoring results of the Jungapeo landslide. (a) Vertical and horizontal accumulated displacement. (b) Horizontal and (c) vertical monthly velocity rate calculated for each monitoring period

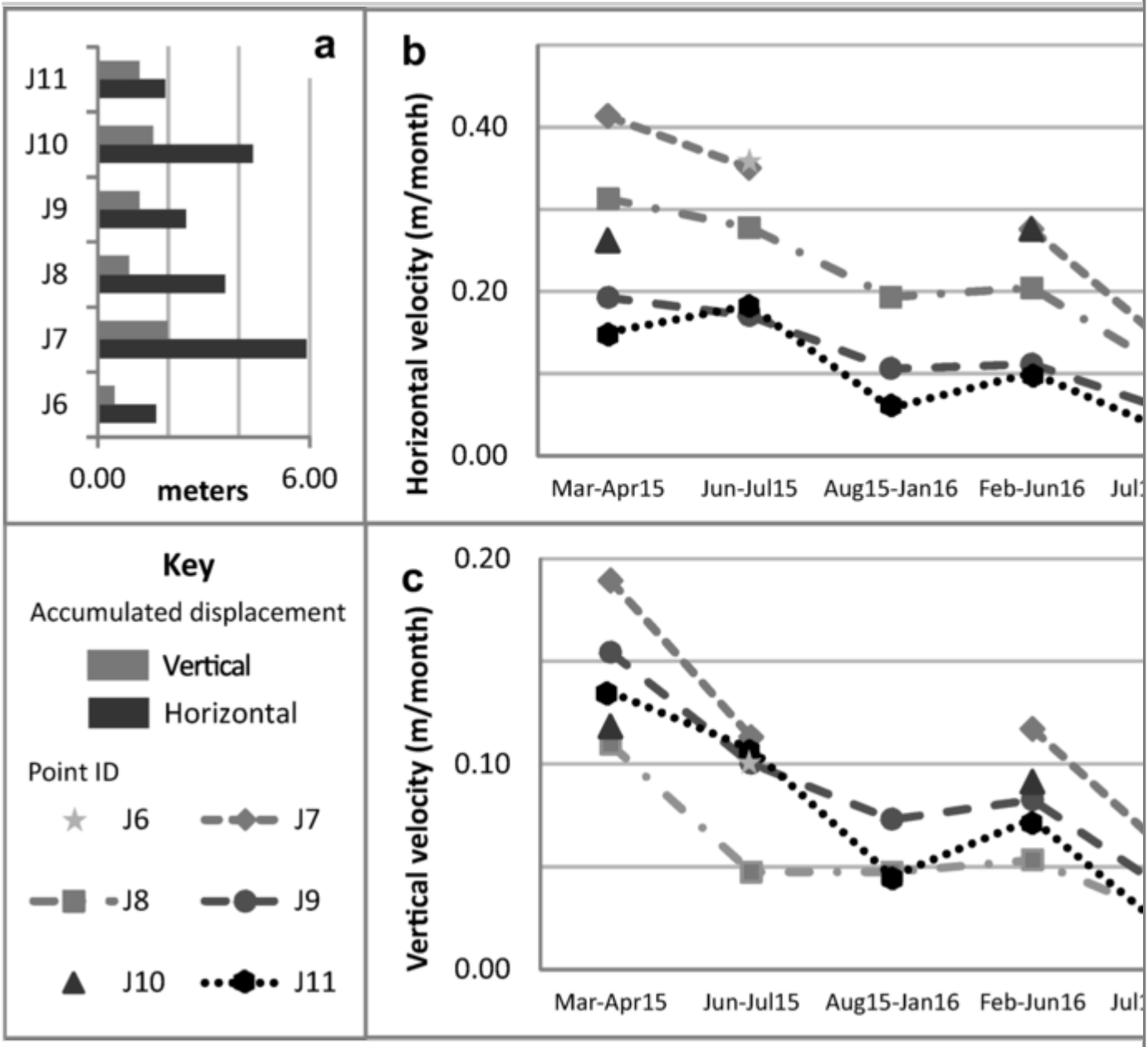

Las Pilas landslide

General characteristics and morphology

The Las Pilas landslide is located on a southwest facing slope, affects an area of approximately 22 Ha and has the perennial Grande River at its toe. Its maximum dimensions are 360 m wide and 700 m long, with a local relief difference of 130 m (1650–1780 m.a.s.l.). It has mobilized a minimum volume of 1,082,467 m^3, estimated with the information from the main scarps of the secondary landslides upon the affected slope. The crown and toe have a slope of 18°–32°, while the middle part ranges from 3° to 17°.

The morpho-structural analysis allowed the delimitation of 19 secondary landslides with a multi-storeyed activity style (Ter-Stepanian 1977) and at least seven deformation stages (Fig. 10). The oldest one produced two large avalanches (up to 650 m in length) that mark the current boundaries of the affected slope. The second stage involved a series of medium-sized landslides, whose boundaries do not interact with each other. It consists of an avalanche (330 m in length with a scarp depth of 10 m), two translational landslides (150 m in length and scarp depths of 5 to 7 m), and three rotational landslides (40 m in length and scarp depths of 2 to 7 m). Stages 3 to 6 developed always in contact with, or directly within the limits of, the landslides of stage 2. These stages include avalanches (430 m in length and a scarp depth of 7 m), translational and rotational landslides that decrease in size (40 to 150 m in length and a scarp depth of 2 to 10 m). The last stage corresponds to small translational landslides (30 m long) and rotational landslides (20 m long) that occurred after the atypical rainfall of 2010.

Fig. 10

Inventory and morpho-structure map of the Las Pilas landslide. At least seven deformation stages with secondary landslide formation were identified

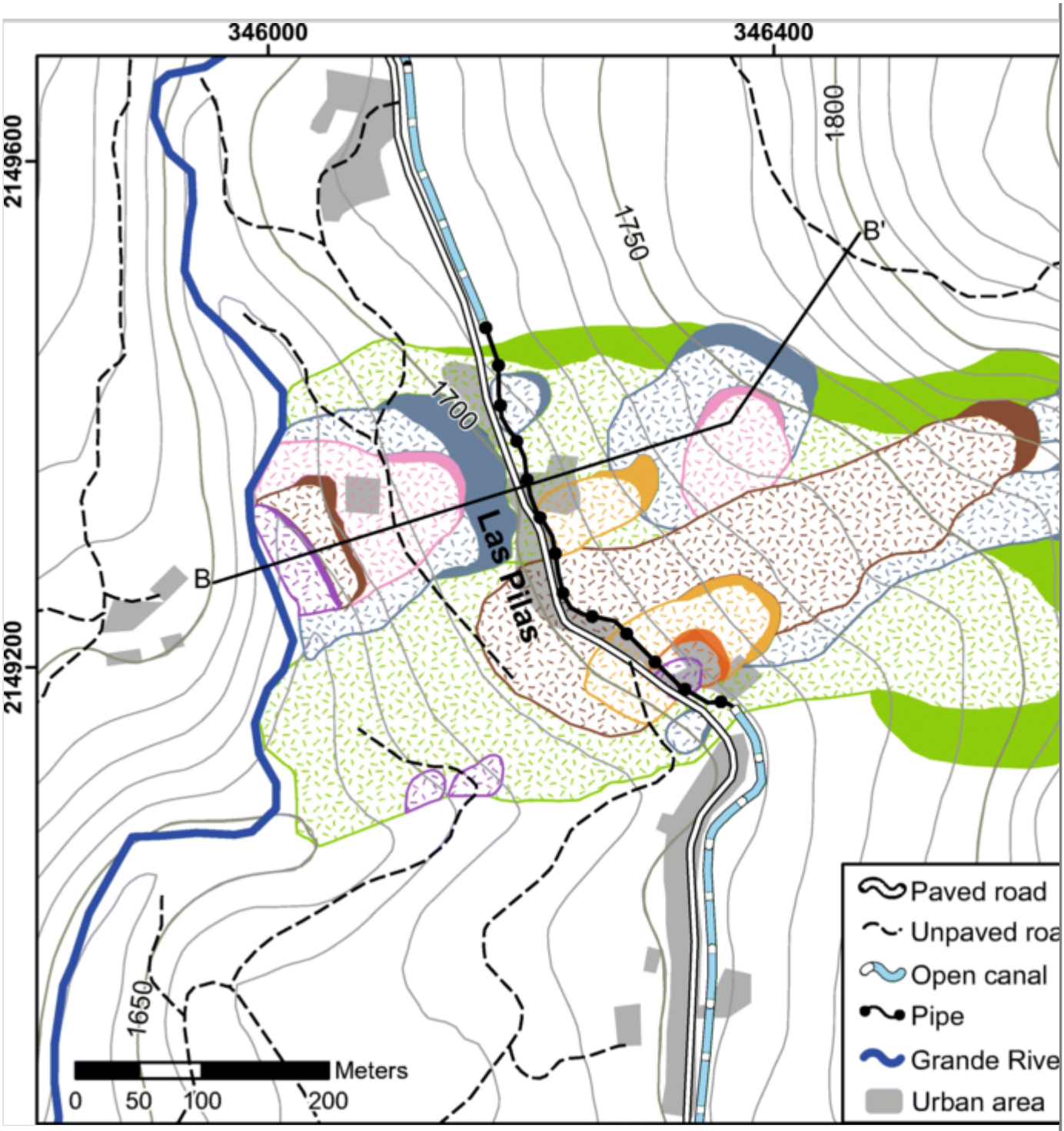

Land use and affectations

Fifty-nine percent of the affected area in Las Pilas is covered by low sub-deciduous forest (8.8 Ha) and pasturelands (4.2 Ha) (F The correct reference is to Fig 12 ig. 12~~0~~). The urban area (1.1 Ha) is perpendicular to the dip of the slope and is located between 1700 and 1710 m.a.s.l. Slow deformation in Las Pilas has taken place at least since the 1940s. The main affected area at that time was the canal that ran parallel to the community, which was highly fractured and had to be piped

(Fig. 11(d)). After the 2010 rainfall occurrence, the movement, which was either in a dormant state or almost imperceptible, began to accelerate. In 2012, a census in the locality revealed that 28 of the 50 house buildings had significant structural damage (Fig. 11). Moreover, the lower part of the slope is covered by chayote and guava crops (7.9 Ha) that have a flood-irrigation system.

Fig. 11

Damage in diverse buildings of Las Pilas village registered in 2012. (a) Vertical and 45° fractures caused by differential movement. (b) Flexion of reinforced column triggering fractures and separation within the wall. (c) Flexion and fractures at 45° in a reinforced column. (d) Separation of at least 70 cm in the wall of the former canal. (e) Small secondary landslide, earth flow, and fractures affecting part of the local church

Surface deformation

Control points P3, P5, and P11, from the DGPS survey, are virtually stable (Fig. 12) and indicate that the deformation does not extend beyond the limits established in the inventory map (Fig. 10). The sectors with displacement (P2, P4, P6–P9) have vectors parallel to the slope-dip direction (N250°), with the exception of P10 (N195°). At this site, the vector seems to be influenced by the topography of the left flank of the DSGSD through which a major irrigation canal also passes.

Fig. 12

Land use and DGPS monitoring network (J2–J14) in the Las Pilas landslide. The size of the displacement vector is proportional to its accumulated movement (black arrows)

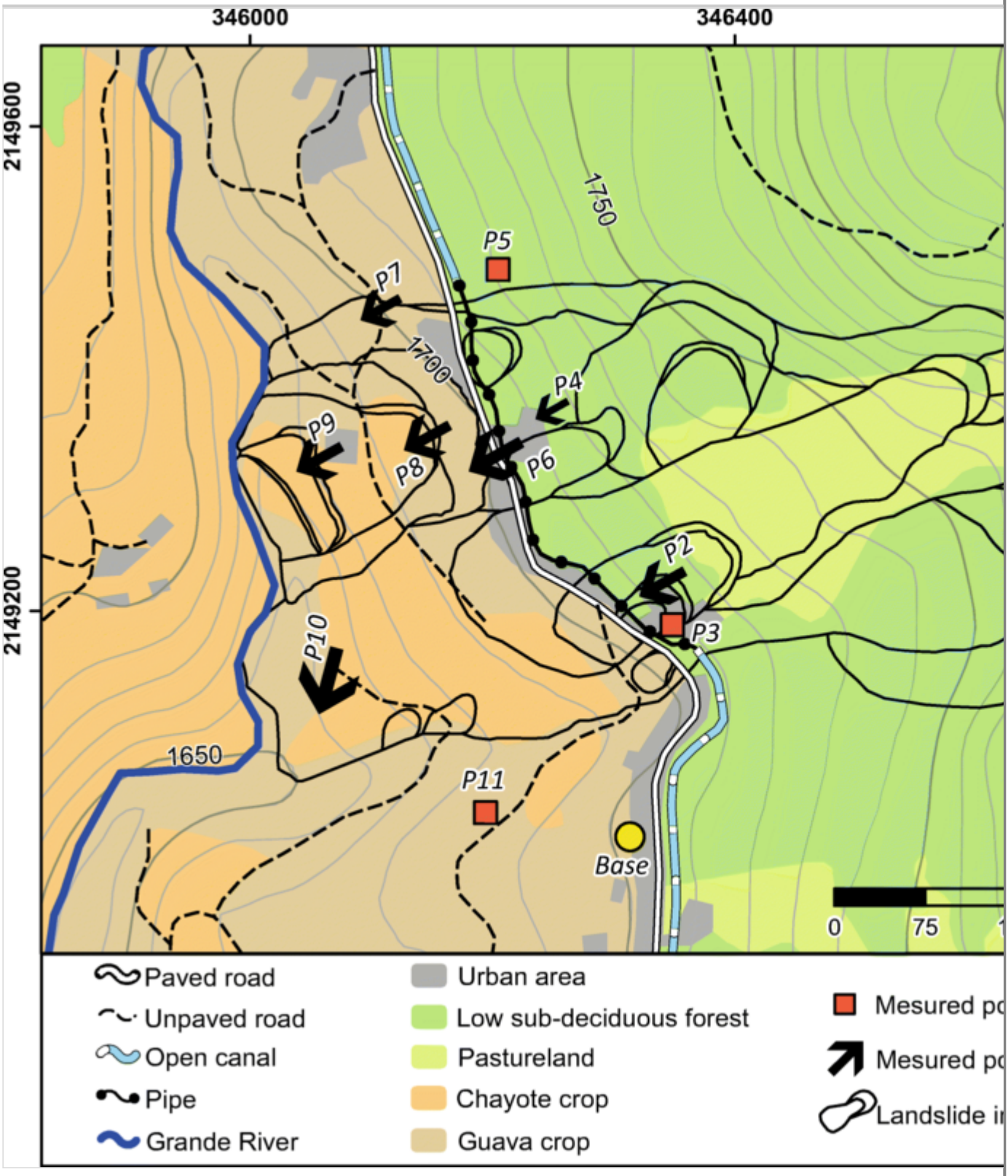

The accumulated displacement values show that all points had vertical and horizontal movements, the latter being predominant in all cases (Fig. 13(a)). The first DGPS displacement rate represents an average for a period of a year and 7 months that does not reflect seasonal changes in behavior (Fig. 13(b, c)). However, the subsequent data shows that horizontal rates range from 1.3 to 0.1 cm/month and have a steady and cyclical behavior. This resembles that which we have observed in Jungapeo with an increase in displacement rates in the first half of the year but decreasing in the second. On the other hand, the range of the vertical rate had a peak in May–June 2015 (1.3 to 0.4 cm/month) that decreased and remained stable for the rest of the monitoring period (0.4 to 0.01 cm/month). This is probably related to the less steep slope.

Fig. 13

DGPS monitoring results in the Las Pilas landslide. (a) Vertical and horizontal accumulated displacement. (b) Horizontal and (c) vertical monthly velocity rate calculated for each monitoring period

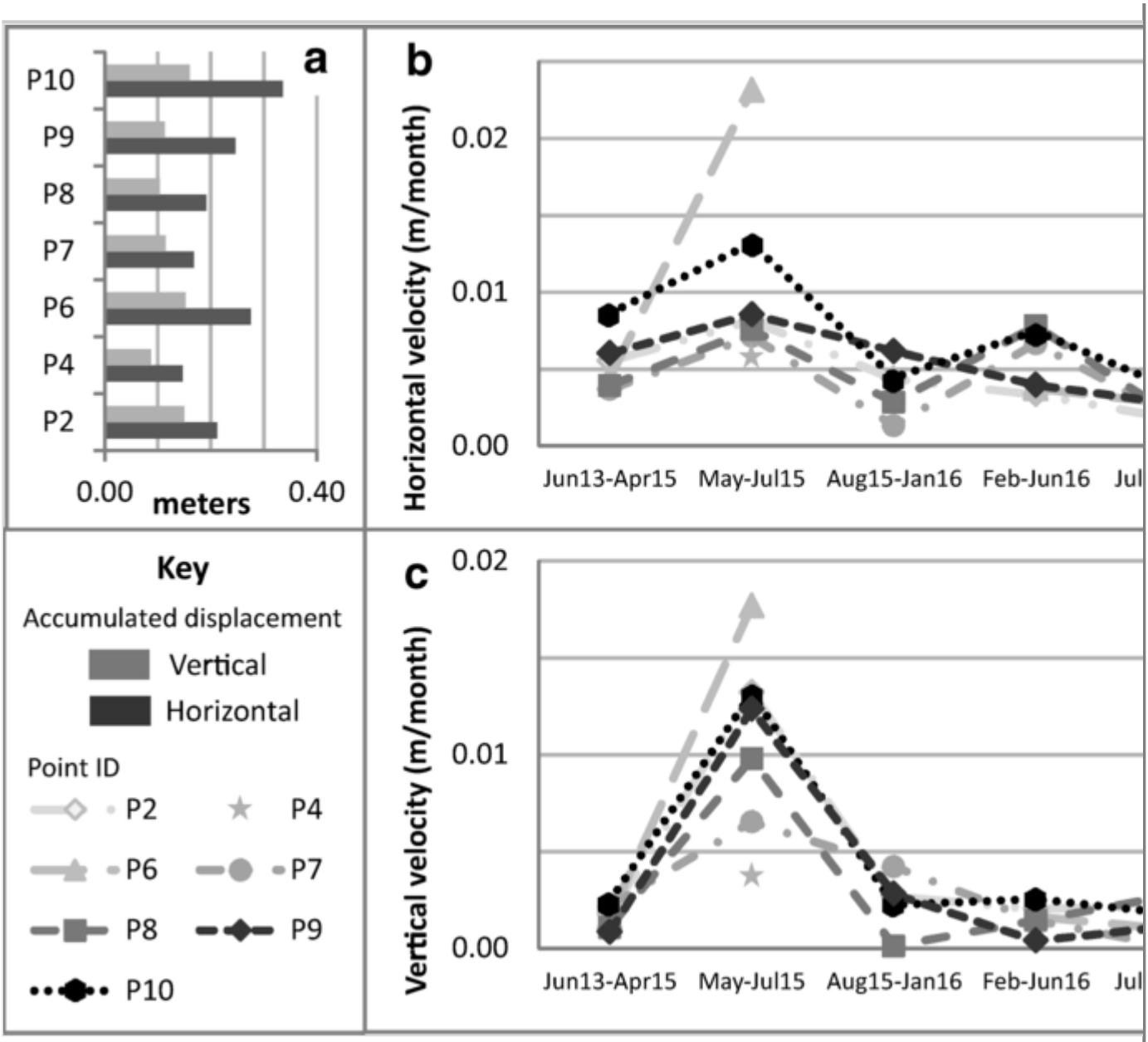

Pluviometric regime

The Jungapeo region has a tropical climate, normally with rainfall during June to September that ranges from 800 to 1300 mm annually and minor rainfall in autumn and winter (Fig. 14; INEGI 2009). For the periods of 1943–2009 and 2011–2015, the rainy season had a frequency of up to 15 days/month with a uniform amount of accumulated rain. Thereafter, the autumn was characterized by a gradual decrease in frequency and amount of rain. In winter, the record indicates a frequency of 1 to 2 days/month. However, January is the month with the highest accumulated rain of this season, while in February and March, it is almost non-existent.

Fig. 14

Accumulated monthly rainfall behavior in station number 16058 of CONAGUA. The asterisk (*) indicates average

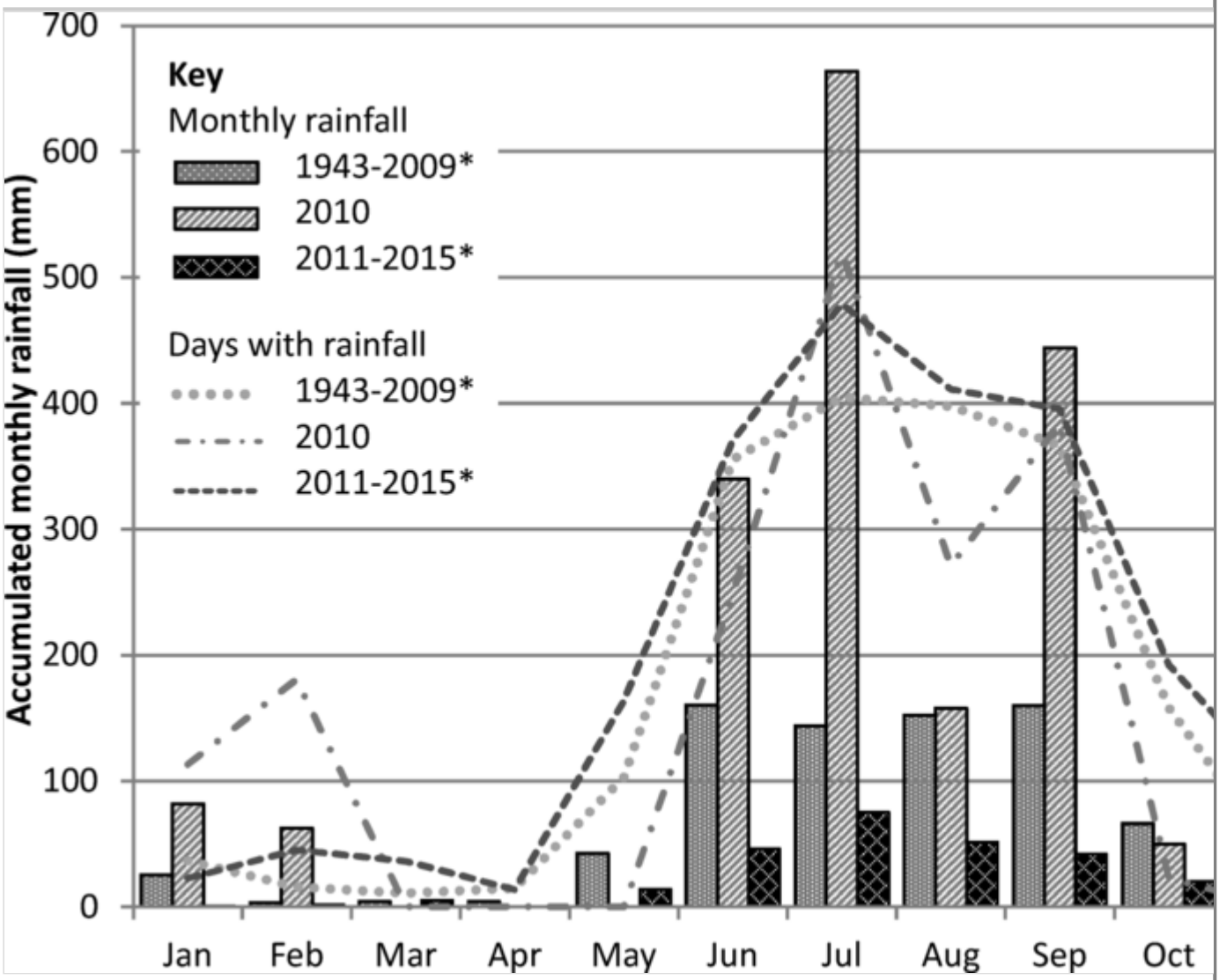

In comparison, what characterized 2010 was the combination of atypical January and February rainfall (82 and 63 mm, respectively) brought on by two cold fronts that interacted with the jet stream and other climatic phenomena (Aguilar-Garduño et al. 2010). Of the total number of years analyzed, the only ones that exceed this amount of rainfall in January are 1967 and 1980, with 118 and 163 mm, respectively. However, the February rainfall has no historical comparison. The highest peak recorded was 28 mm in 1968, almost half of the estimate for 2010. On the other hand, the rainy season (excepting August) also presented accumulated values above the average. The months of June, July, and September represent an increase of 112, 362, and 177% with respect to the period of 1943–2009.

The pluviometric regime of 2010 in eastern Michoacan had a behavior with no previous instrumental record. The duration and amount of rain triggered an acceleration of the slow deformation evolving in collateral landslides on both slopes. In another aspect, the displacement during the second half of the year is related to the seasonal and autumn rains. However, the higher rates during the first half of the year do not show a correlation with the pluviometric regime. Thus, this indicates the existence of another dominant triggering factor that promotes the acceleration during the driest season.

Discussion

From the foregoing results, the Jungapeo and Las Pilas landslide deformation history cannot be related only to the fastest and shallow landslides identified. Nonetheless, the extension, the morpho-structural evidence, both old and recent, and the observed rates of deformation define the phenomena as DSGSD (Fig. 15). The slow deformation predisposes the terrain to generate tension cracks and secondary scarps from which the collateral landslides are given rise to, as seen in the left flank of the Jungapeo landslide (Fig. 6). Collateral landslides are thus triggered in a short period by water saturation of the lithologies, that is, mainly the result of anthropogenic activities, for example, the Las Pilas open-canal case in the early 1940s and the atypical rains of 2010 in both communities. One of the main conditioning factors promoting this behavior is the highly expandable materials forming the slopes resulting from the thinly stratified and folded volcano-sedimentary sequence in Jungapeo and the massive clay-rich and poorly cohesive volcanic breccia in Las Pilas, in addition to the significant weathering.

Fig. 15

Geological and morpho-structural cross-sections of Jungapeo (A–A') and Las Pilas landslides (B–B') along the traces depicted in Figs. 6 and 10. Land use and accumulated displacement vectors (black arrows) are referred to in Figs. 8, 9, 12, and 13. Lithology patterns as for Figs. 3 and 5. FCr former crop, SSc secondary scarps

AQ2

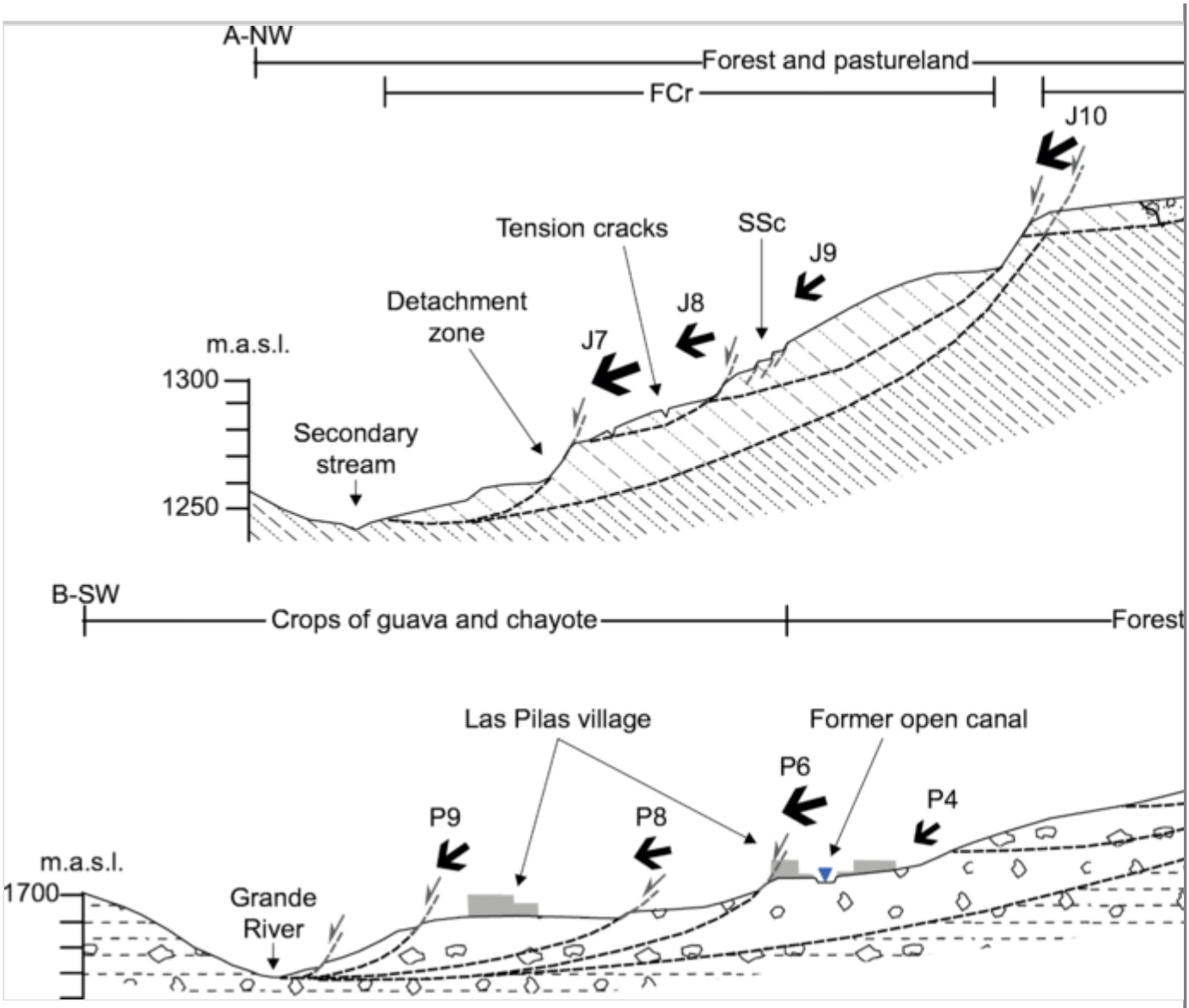

Land use, especially agricultural irrigation areas, has proven to have a twofold implication that is behaving both as conditioning and triggering factors on the affected slopes. As a conditioning factor, it nurtures the relationship between crops and landslide occurrence as has been documented in other places by DeGraff and Canuti (1988) and Gorokhovich et al. (2013). According to testimonies of the inhabitants, the area on which the currently affected sports ground is located in the Jungapeo landslide was donated after a landslide destroyed the orchard that had been there. Additionally, following the atypical 2010 rainfall, not just the left flank affected by cracks and secondary scarps but the entire central part, which once contained an important guava cultivation, led up to secondary landslides (Figs. 8 and 15(A-A')).

The gradual reduction of the velocities in the Jungapeo landslide corresponds to the expected behavior after an acceleration stage caused by an atypical rainfall event

(Pánek and Klimeš 2016). However, the cyclical behavior of acceleration of the velocities during the first half of the year does not correlate with the rainy season in the area (June–September), despite the difference between the magnitudes of the deformation of both slopes. It is also noteworthy here that in the first semester of the year, the amount of rainfall and the number of days over which it occurs are less than half of that recorded for the second semester, even after taking into account completely atypical years, such as 2010 (Table 1).

Table 1

Accumulated rainfall behavior of the first and second semester (average*) in the Jungapeo area

		1943–2009*	2010	2011–2015*
First semester	Monthly rain (mm)	241	485	70
	Rainy days	24	24	29
Second semester	Monthly rain (mm)	550	1316	199
	Rainy days	61	53	71

However, it is broadly recognized that other kind of landslides, such as flowslides, are especially prone to developing in agricultural areas, where the irrigation systems are the main triggering factor (Li et al. 2013; Zhang and Wang 2017). After an intensive expansion of perennial monocultures in Jungapeo in the 1980s, the water demand for the dry season, that is, the first half of the year, increased considerably. Nearly 93% of farmers in the region use the inefficient flood-irrigation system, where 40% of all the water flowing through uncoated canals is lost (Mendoza-López et al. 2005). The use of these uncoated canals occurs at the start of the rainy season in February and ends in June. Consequently, unlike a spatially distributed rainfall, constant saturation and excess water in specific parts of the slope promote the atypical acceleration reflected in the DGPS measurements. Conversely, the extension of crops also plays a vital role as depicted in Fig. 15. For example, in the Las Pilas landslide, where the entire lower part of the slope is occupied by crops under a flood-irrigation system, the cyclical behavior has not decreased (Fig. 15, (B–B')). In comparison, however, the remnant crops in the central part of the Jungapeo landslide are smaller and have a drip-irrigation system (Fig. 15, (A–A')). Nonetheless, the same behavior is observable here although to a lesser extent.

Conclusions

We have described, monitored, constrained, and characterized two recent geomorphological events as deep-seated gravitational slow deformations (DSGSD), in Jungapeo and another in Las Pilas, both in Michoacan, Mexico. Our results show that very slow rates of deformation and a multi-storeyed style of activity have characterized both landslides. The conditioning internal factors for slow deformation in both DSGSD are the combination of thinly stratified and deformed basement rocks. These rocks are severely weathered and possess a clay- and sand-rich content on relatively steep slopes of up to 40°. External conditioning factors include the local shift toward intensive monoculture. Contrary to what should be expected, we have found that the excess water dripped to the soil by the inefficient irrigation system serves to trigger the atypical acceleration behavior during the dry season.

Further, secondary landslides developed from tension cracks and secondary scarps show a definite relation to the DSGSD activity and were triggered by events of extraordinary rainfall, such as the 2010 event. The concurrent development of tension cracks and secondary scarps, and the activity of the detachment zone in the central part of the Jungapeo landslide might contribute to the development of another acceleration stage if a rainfall event similar to that of 2010 should occur. It is important to note here that the accumulated speed and movement in the Las Pilas landslide are constant but smaller than those in Jungapeo. However, the abundant agricultural areas in the former have prevented both their accumulated speed and movement from decreasing. Thus, in the event of sudden collapse, the calculated rock volume (990,455 m^3 in Jungapeo and 1,082,467 m^3 in Las Pilas) would represent a potentially grave risk to each community. Finally, the existence of a perennial river at the foot of each DSGSD implies further that the creation of a potential dam would also endanger other nearby towns.

Acknowledgements

We thank the Comisión Nacional del Agua for providing the data of the meteorological stations. The authors would like to thank the editor and the anonymous reviewers for their accurate comments that highly improved the quality of the manuscript. ~~Thanks to CONACYT project CB-2009-01 and project CIC-UMSNH 2015 and 2016.~~

Funding information

This work is part of PhD project at Instituto Potosino de Investigación Científica y Tecnológica, Mexico, financed through scholarship number 259284 by CONACYT. This research was partially funded by~~financially supported~~ CONACYT project CB-2009-01 and project CIC-UMSNH 2015 and 2016. ~~by CONACYT through Ph.D. scholarship number 259284.~~

References

Aguilar-Garduño E, Santillán H, Salgado M, Martínez M (2010) Análisis técnico de la vulnerabilidad hidrológica ante el crecimiento urbano. Caso de Angangueo, Mich. XXI Congreso Nacional de Hidráulica Zapopan Jalisco

Aguirre-Díaz GJ, Jaimes-Viera MC, Nieto-Obregón J (2006) The Valle de Bravo Volcanic Field: Geology and geomorphometric parameters of a Quaternary monogenetic field at the front of the Mexican Volcanic Belt. Geological Society of America Special Paper Penrose Conference Series: 139–154. https://doi.org/10.1130/2006.2402(06)

Blatter D, Carmichael I (1998) Plagioclase-free andesites from Zitacuaro (Michoacán), Mexico: petrology and experimental constraints. Contrib Mineral Petrol 132:121–138

DeGraff JV, Canuti P (1988) Using isopleth mapping to evaluate landslide activity in relation to agricultural practices. Bull Int Assoc Eng Geol 38:61–71. https://doi.org/10.1007/BF02590449

Figueroa-Miranda S (2013) Estudio del peligro por flujos de detritos y corrientes hiperconcentradas mediante Simulación Numérica en Flo-2d, caso de estudio: Angangueo, Mich. MS Thesis, Universidad Michoacana de San Nicolás de Hidalgo, Michoacán, Mexico

Garduño VH, Corona P, Israde I, Arreygue E, Mennella L, Bigioggero BY, Chiesa S (1999) Carta Geológica del Estado de Michoacán. Secretaría de Difusión Cultural y Extensión Universitaria, Universidad Michoacana de San Nicolás de Hidalgo, Morelia, Michoacan, Mexico, scale 1:250000

Gorokhovich Y, Doocy S, Walyawula F, Muwanga A, Nardi F (2013) Landslides in Bududa, Eastern Uganda: preliminary assessment and proposed solutions. In: Margottini C, Canuti P, Sassa K (eds) Landslide science and practice, volume 4:

global environmental change. Springer, Berlin, pp 145–149. https://doi.org/10.1007/978-3-642-31337-0_19

INEGI (2009) Jungapeo, Michoacán de Ocampo. Clave geoestadística 16047. Prontuario de Información Geográfica Municipal de los Estados Unidos Mexicanos

INEGI (2010a) Censo de Población y Vivienda 2010 [WWW Document]. URL http://www.beta.inegi.org.mx/proyectos/ccpv/2010/ . Accessed 1 Jan 17

INEGI (2010b) Norma Técnica de Estándares de Exactitud Posicional [WWW Document]. URL http://www.inegi.org.mx/geo/contenidos/normastecnicas/doc/norma_tecnica_sobre_es . Accessed 1 Jan 17

Israde-Alcántara I, Martínez L (1986) Contribución al estudio geológico de la transición Pacífico-Tethis en el área de Zitácuaro, Michoacán. BS Thesis, Instituto Politecnico Nacional, Mexico City, Mexico

Li T, Zhao J, Li P, Wang F (2013) Failure and motion mechanisms of a rapid loess flowslide triggered by irrigation in the Guanzhong irrigation area, Shaanxi, China. In: Wang F, Miyajima M, Li T, Shan W, Fathani TF (eds) Progress of geo-disaster mitigation technology in Asia. Springer Berlin Heidelberg, Berlin, pp 421–433. https://doi.org/10.1007/978-3-642-29107-4_24

Mendoza-López MR, Luis-Aguilar A, Castillo-Orta SF, Vidales-Fernández I (2005) Diagnostico del manejo actual del cultivo de guayaba en la region Oriente de Michoacán. Cent Investig del Pacífico, INIFAP 57

Muñiz-Jauregui JA, Hernández-Madrigal VM (2012) Zonificación de procesos de remoción en masa en Puerto Vallarta, Jalisco, mediante combinación de análisis multicriterio y método heurístico. Rev Mex Ciencias Geol 29:103–114

Pánek T, Klimeš J (2016) Temporal behavior of deep-seated gravitational slope deformations: a review. Earth-Sci Rev 156:14–38. https://doi.org/10.1016/j.earscirev.2016.02.007

Pasquarè G, Ferrari L, Garduño-Monroy VH, Tibaldi A, Vezzoli L (1991) Geology of the central sector of the Mexican Volcanic belt, States of Guanajuato

and Michoacán. Geol Soc Am Map Chart Ser MCH072 22

Ter-Stepanian G (1977) Types of compound and complex landslides. Bull Int Assoc Eng Geol 16:72–74

Zhang F, Wang G (2017) Effect of irrigation-induced densification on the post-failure behavior of loess flowslides occurring on the Heifangtai area, Gansu, China. Eng Geol 236:111–118. https://doi.org/10.1016/j.enggeo.2017.07.010